

Absorption in GaAs/Ga_{1-x}Al_xAs quantum wells with resonant barriers for improved responsivity

M. S. Kiledjian, J. N. Schulman,* and K. L. Wang
 Device Research Laboratory, Department of Electrical Engineering,
 University of California at Los Angeles, Los Angeles, California 90024-1594
 (Received 22 March 1991)

We have devised a modified GaAs quantum-well structure with high responsivity. The modification includes putting small barriers on the sides of the quantum well to increase absorption from the bound to an extended state, thus optimizing device performance by increasing the amplitude of the extended-state wave function in the well region. The width and the height of the barriers can be modified to control the spectrum of absorption. The analysis was done using a two-band tight-binding method to calculate the wave functions. The results indicate that, in general, the bigger and the wider the barriers, the narrower and the larger the absorption is, and the stronger the resonance becomes.

I. INTRODUCTION

Recently, there has been great interest in quantum-well infrared detectors.¹⁻⁸ One possibility for infrared detection using GaAs quantum wells involves intersubband absorption between bound states. The quantum wells are designed to have two bound states separated by an energy corresponding to the wavelength of the light to be absorbed. The light is strongly absorbed because of the large oscillator strength, with a relatively high selectivity of $\Delta\lambda/\lambda \approx 10\%$. The excited state is chosen close to the top of the well, and the excited electrons tunnel out in order to escape. An applied voltage across the structure must be sufficiently large to allow the excited electrons to tunnel out, but too large a voltage also causes undesirable leakage from the bound state. To overcome these difficulties, the interest has shifted towards bound-to-extended-state wells having only one bound state in the well.⁹

In this paper, we investigate a modified version of the bound-to-extended-state quantum-well structure. The well is constructed to have two added barriers on its two sides as in Fig. 1. This idea has been mentioned by various researchers in recent years; this is a systematic calculation of the effect of the modification on the absorption

coefficient and the responsivity. In this calculation, the added barriers used consist of a few layers (about 3-10 layers) of Ga_{1-x}Al_xAs alloy. Their height is controlled by adjusting the Al concentration x . The effect of the added barriers is to impart to the wave function a semi-bound quality over a limited resonant energy range in the continuum. At resonance it will have a bigger amplitude in the well region than without the added barriers. Thus, the overlap integral and the oscillator strength will increase with increasing width or height of the added barriers. This also results in an increase in the absorption peak and the responsivity of the device, as will be shown below.

II. THEORY

A. Absorption

To find the absorption coefficient α , we need the transition rate W , which is given by

$$W = \frac{2\pi}{\hbar} \sum_f |\langle \Psi_f | H_{\text{int}} | \Psi_i \rangle|^2 \delta(E_f - E_i - \hbar\omega), \quad (1)$$

where E_i and E_f are the energies of the electron in the bound and the extended states, respectively.

The well-known interaction potential is¹⁰

$$H_{\text{int}} = \left[\frac{e A_0}{m_0 c} \right] P_z, \quad (2)$$

where A_0 is the vector potential and m_0 is the free-electron mass. In our calculation, the photon wave vector is ignored (dipole approximation), and it is assumed that the incoming photon is polarized along the z direction (perpendicular to the well in the $\langle 001 \rangle$ direction for convenience). Then, the transition rate becomes

$$W = 2 \left[\frac{2\pi}{\hbar} \right] \int d^3k |M_{fi}|^2 \delta(E_f - E_i - \hbar\omega), \quad (3)$$

where

$$M_{fi} \equiv \langle \Psi_f | H_{\text{int}} | \Psi_i \rangle \quad (4)$$

and the factor 2 comes from considering the spin degeneracy ($\times 2$) of the continuum states.

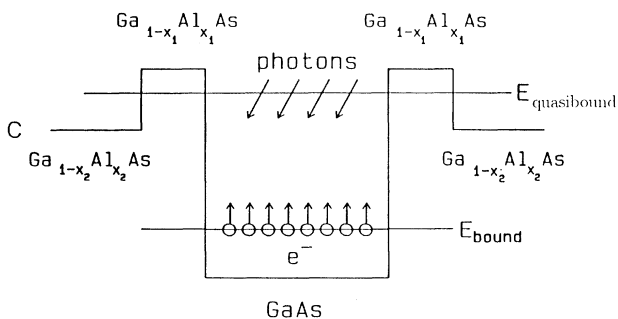


FIG. 1. GaAs quantum well with barriers. The electrons are in the bound state in the conduction band denoted by C. Light entering from the side causes excitations that allow the electrons to escape to the outside. A small bias (not shown) will drive the electrons to the preferred direction.

To determine the transition rate, we use two-band tight-binding wave functions,¹¹

$$\Psi = \sum_l C_s(l)\Phi_s(l) + C_p(l)\Phi_p(l) \quad (5)$$

with the orthonormalization conditions

$$\langle \Phi_{s,p}(l) | \Phi_{s,p}(l') \rangle = \delta_{l,l'}, \quad (6)$$

$$\langle \Phi_s(l) | \Phi_p(l') \rangle = 0 \quad \text{for all } l', \quad (7)$$

where $\Phi_s(l)$ (s -like wave function) is on the l th cation Ga, and $\Phi_p(l)$ (p -like wave function) is on the l th anion As. The coefficients for the wave functions $C_s(l)$ and $C_p(l)$ are found by a transfer-matrix method (starting from one unit cell just to the left of the left barriers and proceeding to one unit cell just to the right of the right barriers).

The two-band tight-binding method is a convenient one for finding the wave functions in these structures. In the tight-binding method, a transfer-matrix method can readily find the coefficients of the wave functions on the individual atoms given the composition and the potential at each atomic location, avoiding the functional complexity due to the applied field in the Schrödinger equation, as is the case for the envelope-function method. Also, the nonparabolicity of the conduction band caused by the $\mathbf{k} \cdot \mathbf{p}$ interaction with the light-hole band is automatically included. The inclusion of the nonparabolicity is important here due to the relatively high energies of the extended states.

The wave functions in the bound and the continuum states are orthonormalized such that

$$\langle \Psi_i | \Psi_i \rangle = 1 \quad \text{for the bound state,} \quad (8)$$

which implies

$$\sum_l |C_s(l)|^2 + |C_p(l)|^2 = 1 \quad (9)$$

and

$$\langle \Psi_{\mathbf{k}} | \Psi_{\mathbf{k}'} \rangle = \delta(\mathbf{k} - \mathbf{k}') \quad \text{for the continuum states.} \quad (10)$$

To do the orthonormalization in the continuum, the quantum-well region along with its double barriers can be

ignored in comparison with the relatively infinite extension of the device.¹² The total wave function (for a given \mathbf{k} value) can be split into two parts, to the left of the left barrier $\Psi_{\mathbf{k}}^L(\mathbf{r})$ and to the right of the right barrier $\Psi_{\mathbf{k}}^R(\mathbf{r})$. Assuming the wave to be traveling from the right to the left, we have¹¹

$$\begin{aligned} \Psi_{k_z}^L(\mathbf{r}) &= \sum_l C_{s,k_z}^L(l)\Phi_s(l) + C_{p,k_z}^L(l)\Phi_p(l) \\ &= \sum_l e^{-ik_z la} [\alpha_{k_z}^L \Phi_s(l) + \beta_{k_z}^L \Phi_p(l)], \end{aligned} \quad (11)$$

where a is the unit-cell length (2.83 Å), $\alpha_{k_z}^L, \beta_{k_z}^L$ are the coefficients of the s and p orbitals on the unit cell $l=0$, to be determined by solving the two-band tight-binding Hamiltonian, and k_z is the wave vector perpendicular to the well of the Bloch wave traveling to the left.

For the wave function on the right side of the right barrier,¹¹

$$\begin{aligned} \Psi_{k_z}^R(\mathbf{r}) &= \sum_l C_{s,k_z}^R(l)\Phi_s(l) + C_{p,k_z}^R(l)\Phi_p(l) \\ &= \sum_l e^{-ik_z la} [m_{1,1}\Phi_s(l) + m_{2,1}\Phi_p(l)] A_i \\ &\quad + e^{ik_z la} [m_{1,2}\Phi_s(l) + m_{2,2}\Phi_p(l)] A_r \\ &= A_i \Theta_{k_z}^i(\mathbf{r}) + A_r \Theta_{k_z}^r(\mathbf{r}), \end{aligned} \quad (12)$$

where $\Theta_{k_z}^i, \Theta_{k_z}^r$ are the incident and reflected Bloch waves; $m_{1,1}, m_{2,1}, m_{1,2}, m_{2,2}$ are coefficients of the s and p orbitals, found by the transfer-matrix method; and A_i, A_r are incident and reflected orthonormalized coefficients of the Bloch waves.

To find M_{fi} we consider the first- and the second-neighbor momentum matrix interactions, and assume Φ_s and Φ_p are real:

$$M_{fi} \equiv \langle \Psi_f | H_{\text{int}} | \Psi_i \rangle = \left[\frac{e A_0}{m_0 c} \right] \langle \Psi_f | P_z | \Psi_i \rangle, \quad (13)$$

with

$$\begin{aligned} \langle \Psi_f | P_z | \Psi_i \rangle &= \sum_l \{ C_s^f(l) * [-C_s^i(l-1) + C_s^i(l+1)] h_s + C_p^f(l) * [-C_p^i(l-1) + C_p^i(l+1)] h_p \\ &\quad + C_s^f(l) * [C_p^i(l-1) + C_p^i(l)] h - C_p^f(l) * [C_s^i(l) + C_s^i(l+1)] h \}. \end{aligned} \quad (14)$$

The second-neighbor interactions between the neighboring cations (h_s) and the neighboring anions (h_p) are given by

$$h_s \equiv \langle \Phi_s(l) | P_z | \Phi_s(l+1) \rangle = - \langle \Phi_s(l+1) | P_z | \Phi_s(l) \rangle, \quad (15)$$

$$h_p \equiv \langle \Phi_p(l) | P_z | \Phi_p(l+1) \rangle = - \langle \Phi_p(l+1) | P_z | \Phi_p(l) \rangle, \quad (16)$$

and the first-neighbor interaction between the adjacent cation-anion pair is

$$\begin{aligned} h &\equiv \langle \Phi_s(l) | P_z | \Phi_p(l) \rangle = \langle \Phi_s(l) | P_z | \Phi_p(l-1) \rangle \\ &= - \langle \Phi_p(l) | P_z | \Phi_s(l) \rangle = - \langle \Phi_p(l-1) | P_z | \Phi_s(l) \rangle. \end{aligned} \quad (17)$$

In the long electron wavelength limit (small k), the $C_s(l)$ and the $C_p(l)$ can be approximated as continuous functions; then h, h_s , and h_p can be determined by requiring consistency with the two-band envelope-function model.

From this we find

$$h_s = h_p = -i\hbar/2a, \quad (18)$$

$$h = -i\sqrt{1/6}m_0P/\hbar, \quad (19)$$

where

$$P \equiv \frac{-i\hbar}{m_0} \langle s | P_z | z \rangle = \sqrt{3E_g\hbar/2m^*}, \quad (20)$$

where E_g is the GaAs or $\text{Ga}_{1-x}\text{Al}_x\text{As}$ band gap, and m^* is the conduction-band effective mass.

Finally, after incorporating M_{fi} in W , the absorption coefficient is calculated by,¹⁰

$$\alpha = \frac{2\pi\hbar c W}{n_r A_0^2 \omega}. \quad (21)$$

The above procedure finds the absorption from the bound- to the excited-state wave functions using the parameters describing the structure (i.e., potential height of the barriers on the two sides, the 2D Fermi level, which is found by knowing the doping concentration, and the effective masses of the electrons in the conduction bands of GaAs and $\text{Ga}_{1-x}\text{Al}_x\text{As}$).

As will be shown, the peak of the absorption does indeed increase with increasing barrier height and width. But an increasing absorption coefficient is not sufficient for optimizing device performance; the ability of the elec-

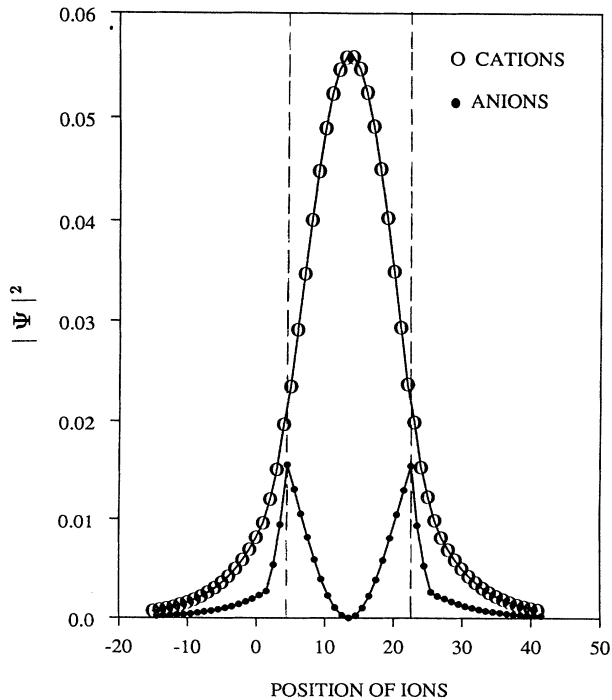


FIG. 2. $|C_s(l)|^2$ and $|C_p(l)|^2$ denoted by circles and solid dots, respectively, for the normalized bound-state energy wave function as a function of atomic position l . Well width = 50.94 Å, barrier width = 8.49 Å, barrier alloy concentration $x_1 = 0.35$, outermost barrier Al concentration $x_2 = 0.15$. The vertical dashed lines represent the well region.

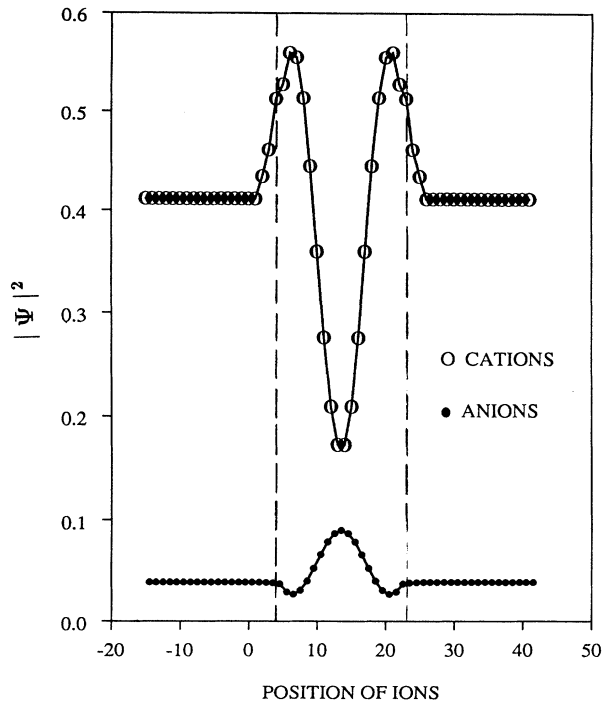
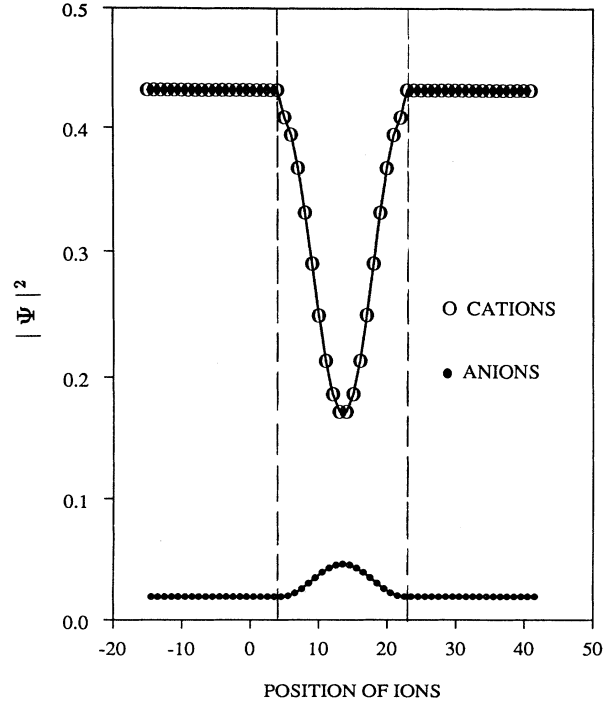


FIG. 3. (a) $|C_s(l)|^2$ and $|C_p(l)|^2$ denoted by circles and solid dots, respectively, for the first normalized quasibound-state wave-function coefficients with no added barriers. Well width = 50.94 Å, outermost barrier Al concentration $x_2 = 0.15$. The vertical dashed lines represent the well region. (b) $|C_s(l)|^2$ and $|C_p(l)|^2$ denoted by circles and solid dots, respectively, for the first normalized quasibound-state wave-function coefficients with added barriers. Well width = 50.94 Å, barrier width = 8.49 Å, barrier alloy concentration $x_1 = 0.35$, outermost barrier Al concentration $x_2 = 0.15$. The vertical dashed lines represent the well region.

trons to tunnel out through the barriers once they are excited and the spectral response of the device must also be considered. It is important to consider the responsivity R , which contains a more complete picture of the device performance. This will be shown in the following section.

B. Responsivity

The responsivity $R(\nu)$ as a function of incident photon frequency ν is given by¹³

$$R(\nu) = \frac{1}{2} \left[\frac{e}{h\nu} \right] g \eta(\nu) \rho(\nu) \quad (22)$$

and

$$\eta(\nu) = 1 - e^{-2\alpha(\nu)w}, \quad (23)$$

where $\eta(\nu)$ is the quantum efficiency, g is the photo-current gain, and the factor 2 accounts for the increased absorption due to the reflection off of a top metallic contact.¹ Further,

$$\rho(\nu) = [1 + \tau_T(\nu)/\tau^*]^{-1}, \quad (24)$$

$$\tau_T(\nu) = \frac{1}{fT(\nu)}, \quad (25)$$

$$f = \frac{v}{2w}, \quad (26)$$

$$v = \frac{2\pi\hbar}{wm^*}, \quad (27)$$

$$g = L/l, \quad (28)$$

where $\rho(\nu)$ is the tunneling escape probability,¹ $\tau_T(\nu)$ is the tunneling escape time, v is the phase velocity of the electron in the resonant state, $T(\nu)$ is the barrier transmission coefficient, τ^* is the photoexcited state lifetime (1 psec is used for this calculation),^{14,15} w is the width of the well, f is the frequency of oscillation inside the quantum well once the electron is excited to the resonant energy in the continuum, L is the hot-electron mean free path, and l is the device length. The factor g is included to account for the transport of the photoexcited carrier through the device. That is, the electron can recirculate through the quantum well via the Ohmic contacts approximately g times. Of course, due to the added resonant barriers, g will be reduced relative to the case without them. For our case, we consider $g = 1$ for simplicity of calculation. Note that the transmission coefficient as a function of frequency $T(\nu)$ must be determined in order to find the responsivity.

III. RESULTS

It is useful to present some representative plots showing typical wave functions. For the case where the well width = 50.94 Å, the barrier width = 8.49 Å, the inner barrier alloy concentration $x_1 = 0.35$, and the outermost barrier Al concentration $x_2 = 0.15$, Fig. 2 shows a plot of the square of the absolute value of the normalized bound-state wave-function coefficients $|C_s(l)|^2$ and $|C_p(l)|^2$ as a function of the atomic locations l . For the first and the only bound-state energy in the well, the wave function is cosinlike as is seen, and it decays exponentially away from the well into the barriers. Figure 3(a) is

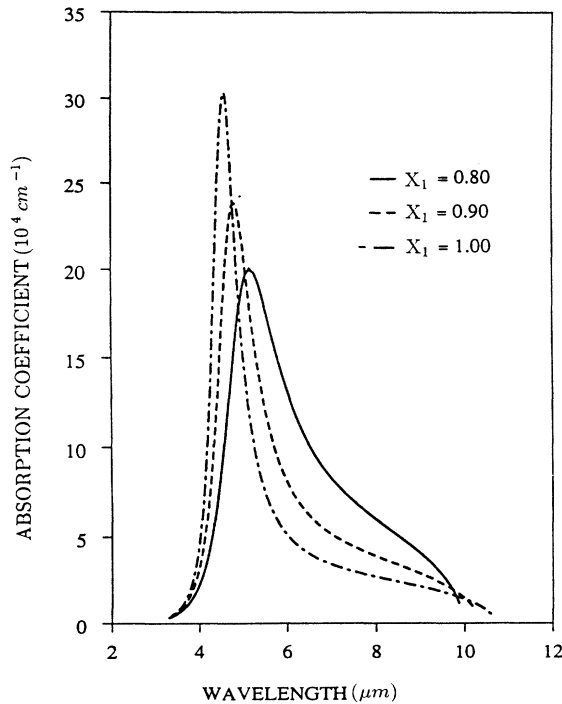


FIG. 4. Absorption α in units of cm^{-1} vs wavelength λ in micrometers of the incident photon for three different barrier heights. (Well width = 50.94 Å, barrier width = 8.49 Å, $x_1 = 0.80, 0.90, 1.00$, and $x_2 = 0.30$.)

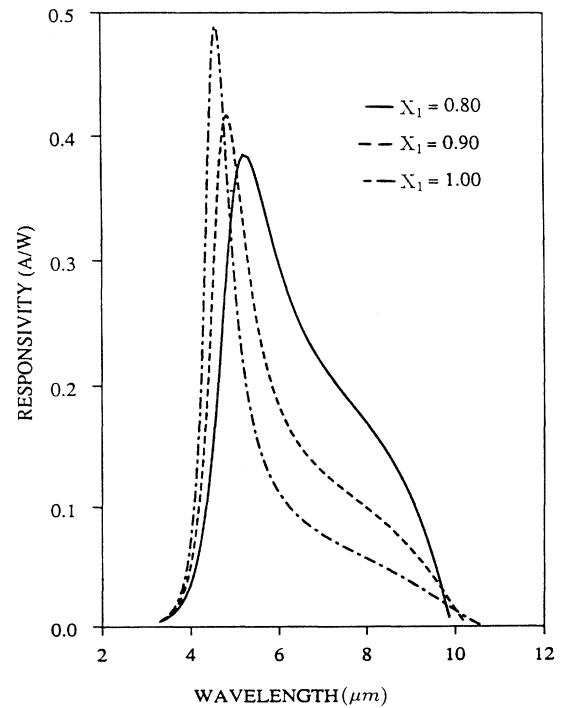


FIG. 5. Responsivity R vs wavelength λ of the incident photon for three different barrier heights. (Well width = 50.94 Å, barrier width = 8.49 Å, $x_1 = 0.80, 0.90, 1.00$, and $x_2 = 0.30$.)

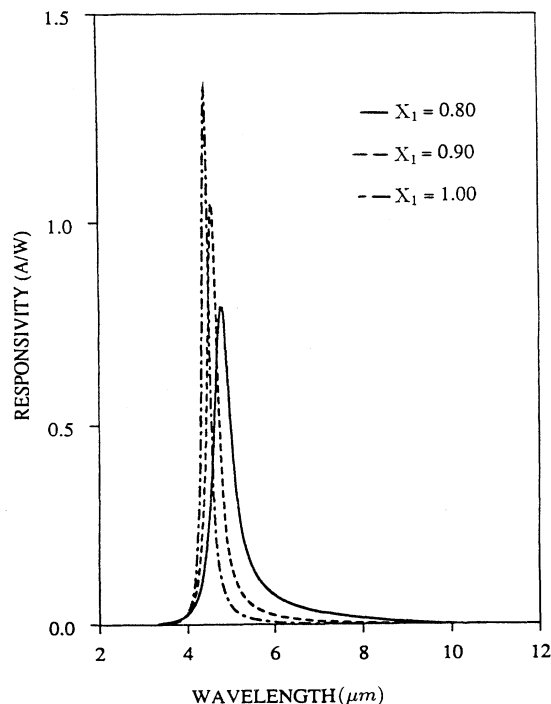


FIG. 6. Responsivity R vs wavelength λ of the incident photon for three different barrier heights. (Well width = 50.94 Å, barrier width = 14.15 Å, $x_1 = 0.80, 0.90, 1.00$, and $x_2 = 0.30$.)

the plot of the first quasibound-state wave function in the continuum (located from the peak in the transmission versus energy) for the same well width (= 50.94 Å) without the added barriers; i.e., with the equal innermost and outermost barrier Al concentration, $x_1 = x_2 = 0.15$. For comparison, also shown in Fig. 3(b) is the plot of the wave function of the quasibound state for the same well width as in Fig. 3(a) but with the added barriers of alloy concentration $x_1 = 0.35$. It clearly demonstrates the increase of the wave function's amplitude with the added barriers.

Figure 4 shows a plot of the absorption coefficient versus photon wavelength for a well width of 50.94 Å and an inner barrier of width 8.49 Å, taking the inner barrier height as a parameter controlled by the barrier alloy concentration x_1 ($x_1 = 0.80, 0.90, 1.00$). A Fermi level consistent with a doping level of $1.0 \times 10^{18} \text{ cm}^{-3}$ in the well is always assumed. With increasing barrier height the curve peak shifts slightly towards the left (higher quasibound energy or shorter wavelength) and it increases in magnitude. Figure 5 shows a plot of R versus wavelength for the same structure as in Fig. 4. These peaks also increase with increasing barrier height. In both cases the halfwidth [full width at half maximum (FWHM)] decreases as expected, indicating greater wavelength selectivity.

Further, to investigate the trend by the widening of the barriers, Fig. 6 shows a plot of R vs λ for the same well width and the same barrier heights as in Fig. 5, but the barrier width is allowed to increase to 14.15 Å. Increasing the barrier width sharpens the corresponding curves

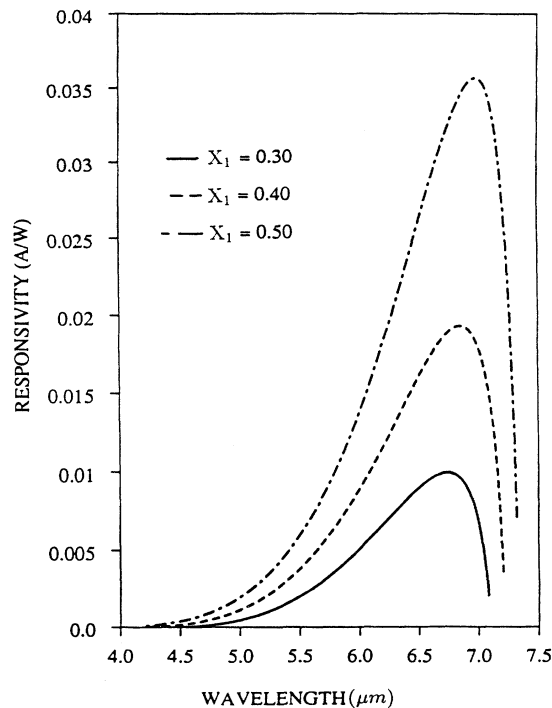


FIG. 7. Responsivity R vs wavelength λ of the incident photon for three different barrier heights. (Well width = 70.75 Å, barrier width = 8.49 Å, $x_1 = 0.30, 0.40, 0.50$, and $x_2 = 0.30$.)

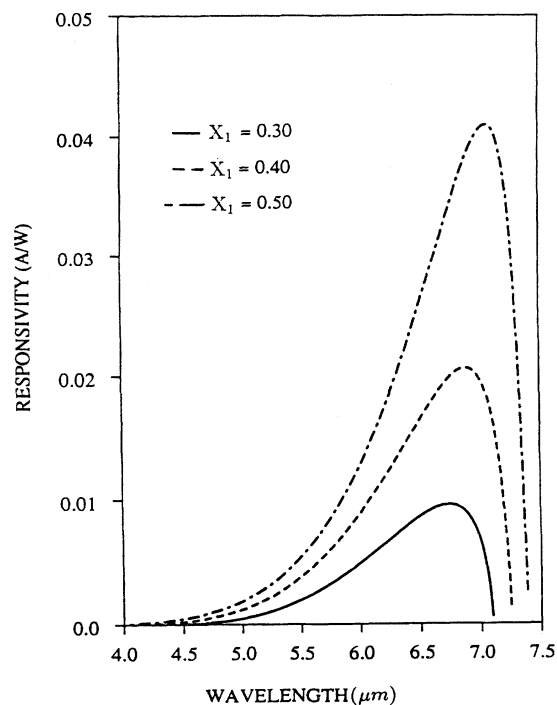


FIG. 8. Responsivity R vs wavelength λ of the incident photon for three different barrier heights. (Well width = 70.75 Å, barrier width = 14.15 Å, $x_1 = 0.30, 0.40, 0.50$, and $x_2 = 0.30$.)

(decreasing FWHM) and enhances their heights.

The same procedure was also applied to a bigger well of width 70.75 Å, and similar results were obtained. Figure 7 shows the responsivity curves for three different barrier heights with alloy concentration x_1 ($x_1 = 0.30, 0.40, 0.50$) with the same barrier width of 8.49 Å. Again, the responsivity increases with barrier height. Also, in Fig. 8, the responsivity curve is enhanced and sharpened for the case with a wider barrier width of 14.15 Å, given the same well width and barrier heights as in Fig. 7. Note that both Figs. 7 and 8 include the case with no barriers ($x_1 = 0.30$). For the curves shown in Figs. 4–8, the outermost barrier's Al concentration x_2 is kept constant ($= 0.30$).

IV. DISCUSSION

It is observed that putting small barriers on the two sides of the quantum well can enhance the absorption coefficient as well as the responsivity of the device. The increase in absorption results also in an increase in the quantum efficiency of the device η . It is interesting to note that even though the tunneling probability ρ decreases with increasing barrier dimensions, this decrease is much slower than the increase in absorption and quantum efficiency; in fact, ρ is generally on the order of uni-

ty. The reason for this is the fact that the photoexcited state lifetime τ^* is much longer than the tunneling escape time $\tau_T(\nu)$ at resonance (approximately two to three orders of magnitude larger) for the barriers considered here, except when the resonant state is very close to the top of the well, in which case $\tau_T(\nu)$ is infinitely large.^{14,15} This allows the electrons sufficient time to escape through the barriers once they are excited without falling back to the bound state. This is an important reason why this modification in the device will enhance the current produced.

V. CONCLUSION

In summary, it is possible to construct quantum-well devices with additional double barriers such that increasing the barrier width and height leads to an improvement in the responsivity as well as the efficiency of the device. A control over the width of the responsivity spectrum for the bound-to-extended-state absorption for infrared detection can also be achieved.

ACKNOWLEDGMENT

One of us (M.S.K.) thanks Dr. R. P. G. Karunasiri for helpful discussions on absorption.

*Also at Hughes Research Laboratories, Malibu, CA 90265.

¹B. F. Levine, K. K. Choi, C. G. Bethea, J. Walker, and R. J. Malik, *Appl. Phys. Lett.* **51**, 934 (1987).

²L. C. West and S. J. Eglash, *Appl. Phys. Lett.* **46**, 1156 (1985).

³B. F. Levine, R. J. Malik, J. Walker, K. K. Choi, C. G. Bethea, D. A. Kleinman, and J. M. Vandenberg, *Appl. Phys. Lett.* **50**, 273 (1987).

⁴A. Harwit and J. S. Harris, Jr., *Appl. Phys. Lett.* **50**, 685 (1987).

⁵A. Seilmeier, H. J. Hübner, G. A. Abstreiter, G. Weimann, and W. Schlapp, *Phys. Rev. Lett.* **59**, 1345 (1987).

⁶K. K. Choi, B. F. Levine, R. J. Malik, J. Walker, and C. G. Bethea, *Phys. Rev. B* **35**, 4172 (1987).

⁷L. Esaki and H. Sakaki, *IBM Tech. Discl. Bull.* **20**, 2456 (1977).

⁸J. S. Smith, L. C. Chiu, S. Margalit, A. Yariv, and A. Y. Cho,

J. Vac. Sci. Technol. B **1**, 376 (1983).

⁹B. F. Levine, C. G. Bethea, K. K. Choi, J. Walker, and R. J. Malik, *J. Appl. Phys.* **64**, 1591 (1988).

¹⁰F. Bassani and G. P. Parravicini, *Electronic States And Optical Transitions in Solids*, 1st ed. (Pergamon, New York, 1975), Vol. 8, pp. 149–154.

¹¹J. N. Schulman, *J. Appl. Phys.* **60**, 3954 (1986).

¹²L. D. Landau and E. M. Lifshitz, *Quantum Mechanics*, 3rd ed. (Pergamon, New York, 1977), Vol. 3, pp. 62 and 63.

¹³B. F. Levine, C. G. Bethea, K. K. Choi, J. Walker, and R. J. Malik, *Appl. Phys. Lett.* **53**, 231 (1988).

¹⁴K. W. Goossen and S. A. Lyon, *Appl. Phys. Lett.* **47**, 1257 (1985).

¹⁵K. W. Goossen and S. A. Lyon, *J. Appl. Phys.* **63**, 5149 (1988).